OPTICAL FIBER TECHNOLOGY **2**, 216-224 (1996)
ARTICLE NO. 0027

Mechanical Reliabilty of $LiNbO_3$ Optical Modulators Hermetically Sealed in Stainless Steel Packages

HIROSHI NAGATA AND NAOKI MITSUGI

Optoelectronics Research Division of the Central Research Laboratories, Sumitomo Osaka Cement Co.,Ltd., 585 Toyotomi-cho, Funabashi-shi, Chiba 274, Japan

Received February 7, 1996

The mechanical reliability of hermetically sealed $LiNbO_3$ (LN) Mach-Zehnder optical intensity modulators is proved. The modulators are packaged in stainless steel cases, instead of conventional Kovar ones sealed by resin materials. Furthermore, in the package, a newly developed adhesive material is also used for butt-coupling of the optical fiber to the LN waveguide. The reliability tests following a Bellcore TR-NWT-000468 standard demonstrate that these unconventional materials used in packaging will not cause any mechanical failures during ordinary device operation. Especially notable is the fact that, although a large mismatch in the thermal expansion of the stainless steel and glass fiber exists, there are no fiber breaks and no optical transmission failures generated by the thermal shocks. © 1996 Academic Press, Inc.

1. INTRODUCTION

Because of a rapid increase in the applications of $LiNbO_3$ (LN) modulator devices to optical transmission and measurement systems, pigtailed fiber/LN packaging technology must now satisfy high standards of mechanical reliability, such as Bellcore's TR-NWT-000468, for use in interoffice optical-electrical systems. Concerning LN packaging strategy, two different methods are proposed: one package is lightly sealed by resin materials and the other is tightly sealed in metals. As an example of the former, a compact surface-mounted Kovar package with co-fired, ceramic, electrode-feed-throughs applied to 2.5-10 Gb/s LN modulators [1,2]. Such technology reduces the cost of packaging, avoiding such materials as metallized fiber, specially designed housings, and a seam-welding processes, which are needed for the tightly sealed packages. Because generally the fiber pigtail is butt-coupled solidly to the LN waveguide by an adhesive material, instead of a lens coupling, the optical transmission is reliable enough for operation under an ordinary atmosphere, even through the package sealing is not very tight [1]. However, in order to achieve high reliability in electrical transmission, the package must be tightly sealed by soldering and seam-welding technology. A considerable penetration of moisture causes short circuits through possible electrochemical reactions of electrode materials, a galvanic reaction, for instance. Further, the exposed surface of the optical fiber pigtail might be corroded by the moisture and might ultimately fail. In this regard, the residual moisture in the packaged LN must be less than 5000 ppm, as well as semiconductor lasers (TR-NWT-000468).

Concerning the reliability of resin-sealed LN modulators, a well-detailed report was presented previously from IOC, Ltd.[1]. Some other reports on the LN reliability did not describe enough of the packaging structure, unfortunately [3]. To clarify this point, here the mechanical reliability of the hermetically sealed LN modulators which were fabricated in volume for promising 10 Gb/s uses is reported. In device production, both the quantity produced and the device reliability are important. In this regard, too, the hermetic sealing process is not disadvantageous compared with resin sealing, because the most of the packaging process time is dominated by the time necessary for fiber alignment and curing the epoxy. The present hermetic packaging was accomplished with an all metallic sealing technique using a stainless-steel (AISI 303) case which matched the thermal expansion of the LN material, instead of a conventional Kovar package. The fiber pigtail was butt-coupled to the LN waveguide using a new epoxy adhesive having a refractive index≅1.46, "UV-1100" by Daikin Industries, Ltd. [4], to further reduce the optical return loss. The reliability evaluation of these unconventional materials, the AISI 303 package and new epoxy, is the main purpose of this article. Results show that these materials were acceptable for package constituents and caused no mechanical and functional problems in LN modulators according to Bellcore's reliability tests.

2. DEVICE STRUCTURE

Figure 1 shows the hermetically sealed modulator for 10 Gb/s operation. The size of the package was $L120 \times W15 \times H10$ [mm]. The surface of the stainless steel (AISI 303) package was plated with an inner Ni and an outer Au binary layer. Commercial K-type (SMA) rf connectors (Wiltron Co.) were hermetically assembled to the package by a Sn/Pb soldering

1068-5200/96 $18.00
Copyright © 1996 Academic Press, Inc.
All rights of reproduction in any form reserved.

FIG. 1. Hermetically Sealed $LiNbO_3$ optical modulator with K-type rf-connectors. The length of the package is 120 mm.

technique. The LN modulator chip ($L60 \times W0.8 \times T0.5$[mm]) was bonded to the package using a commercial thermally curable epoxy adhesive material with electroconductive fillers (EpoTek H20E). The details of the Mach-Zehnder LN modulator chip were described in Refs. [5, 6]. The hot electrode of the chip was linked to the K-connector electrode pin via a sliding contact (Wiltron Co.) which was directly bonded to the chip electrode pad by thermo-ultrasonic bonding. A polarization maintaining fiber and a normal single mode fiber were butt-coupled to input and output ends of the LN chip waveguide, respectively, using a commercial ultraviolet(uv) curable epoxy (Daikin UV-1100), as shown in Fig.2 [4]. A glass bead and an LN block were attached to the chip foe reinforcement of the fiber bonding.

Figure 3 shows schematically the structure of the fiber sealing portion with an RMA grade Sn/Pb(60/40) solder. The fiber jacketed with uv-cured resin materials (0.4 mm outer diameter, Fujikura UV-400) was used. These fibers were known to be significantly improved against possible fiber breakage due to thermal contraction of the jacket materials [7, 8]. The glass fiber surface was coated with a Ni layer and further

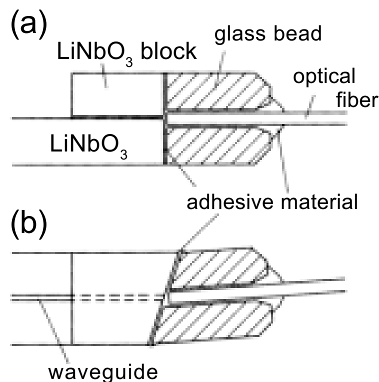

FIG. 2. Schematic illustrations of a bonding structure of optical fiber to LN modulator chip; (a) side view and (b) top view.

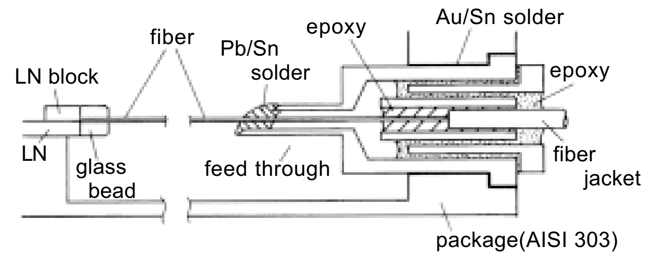

FIG. 3. Schematic cross-sectional illustration of a fiber feed-through structure of the package.

with a Au layer using an electroless plating technique. In order to compensate for thermal expansion difference between the fiber and the package, before the soldering process, the metallized fiber was bent slightly through a ~25 mm distance between the LN and the point where the jacket was removed; the fiber was thrust about 35 μm toward the LN. The gap between the fiber jacket and the package feed-through was filled with a room temperature curable epoxy adhesive. Further, a polyester (hytrel) loose tubing (0.9 mm in a outer diameter), protecting the 0.4 mm diameter fiber, was bonded to a rubber boot fixed to the package fiber feed-through (not shown in Fig. 3). Finally the package lid was seam-welded under a dry N_2/He atmosphere (dew point < -40°C). The consequent He (tracer gas for the fine-leak test) content in the package was measured to be 10-15% by mass spectroscopy. The residual moisture was also measured to be 0.5-1.5% for the similar devices, which had not been baked prior to the packaging process. However, the residual moisture could be reduced 2000-3000 ppm, when the package was baked at 80°C for 15 h under 5 mTorr atmosphere prior to the seam welding process.

The typical parameters of the fully packaged modulators were 3.6 dB optical insertion loss, 46 dB optical return loss, 3.4 V half-wave voltage (V_π), 25 dB on/off extinction ratio, 4.6 GHz electrical bandwidth, and 8.6 GHz optical bandwidth. Further, a thermal stress analysis of the stainless-steel package was carried out, because the 120-mm-long package is to be mounted on a board for the system assembly. Assuming the package was bolted on the $L150 \times W50 \times T20$ [mm] aluminum heat sink, the internal stress of the package was calculated to be a maximum of about 110 Mpa within the temperature increase from 0 to 70°C. This estimated stress was smaller than the 0.2% proof stress (≅ yield point of the material) for the stainless steel (~250 Mpa), indicating that no mechanical problem occurs for the package itself due to the thermal cycles.

3. TEST CONDITIONS

Eleven LN modulators were exposed under successive tests of mechanical shocks at 500 G (MS), heat cycles between -40 and 70°C (HC), low temperature storage at -50°C (LTS), vibrations between 20 and 2000 Hz at 20 G (VB), fiber pulls with 1 kg (FP), and damp heat storage with dc = 5 V application at

TABLE 1
Environmental Test Conditions

Test	Reference	Conditions
Mechanical shock (MS)	MIL-STD-883 2002, A	500 G, 1.0 ms, 5 times/axis
Heat cycle (HC)	MIL-STD-883 1010	-40 ~ +70 ℃, 100 cycles min. rate = 10 ℃/min
Low-temperature storage (LTS)	—	- 50 ℃, 7 days
Vibration (VB)	MIL-STD-883 2007, A	20-2000 Hz, 20 G, 4 min/cycle, 4 cycles/axis
Fiber pull (FP)	—	1 kg, 10 s, 3 times
Damp heat (DH)	IEC-68-2-3	40 ℃, 95%RH, 56 days biased (dc = 5 V here)

40°C and 95%RH (DH). The details of the test conditions are listed in Table 1. After each test, optical insertion loss, optical return loss, V_π, on/off extinction ratio, and electrical and optical bandwidths were measured at a light wave length of 1.5 µm and at ordinary room temperature (25-30°C). During the DH test, optical insertion loss, return loss, V_π, extinction ratio, and electrical resistance between the hot and ground electrodes were measured under the test environment, *i.e.*, 40°C and 95%RH, at the 0th , 4th, 10th, 21st, and 56th day. The other two modulators were placed under laboratory room conditions as a reference sample and measured for the above-mentioned parameters at the time when the tested samples were inspected.

In order to evaluate the package hermeticity, the following tests were conducted: 100 heat cycles between -65 and 150°C (MIL-STD-883, 1010 C), 15 heat shocks between -55 and 125°C (MIL-STD-883, 1011B), and the fine-leak tests. Three types of the package samples were prepared for the tests. The first 5 samples were packaged with a seam-welded lid. The second 10 samples were packaged with two soldered glass beads for rf-electrical connection and a seam-welded lid. The third 9 samples were packaged with two soldered fibers (without jacket materials) and a seam-welded lid. The fine-leak test was carried out by the He-bombing method mentioned in MIL-STD-883, 1014.9, A1.

4. RESULTS OF ENVIRONMENTAL TESTS

Figure 4 to 8 show environmental test-induced changes of optical insertion loss, optical return loss, V_π, on/off extinction ratio, and electrical and optical bandwidths, respectively. In the figures, the circles and error bars mean the averaged values and standard deviations ($\pm\sigma_{n-1}$), respectively. The error bars include a distribution of the measured results dependent on the measurement equipment and the person, *i.e.*, measurement repeatability. Such distribution was, in σ_{n-1} value, 0.5 dB for optical insertion loss, 8.0 dB for return loss, 0.2 V (~6%) for V_π, 5.0 dB for extinction ratio, and 1.0 GHz for bandwidth. The "Ref." in the figures denotes the data for the reference samples without any environmental tests.

In almost all parameters, there was no change greater than those for the reference samples after the environmental tests. Although the data distribution for the insertion loss (Fig.4) and the optical bandwidth (filled circles in Fig. 8) was somewhat larger than the references, it seemed to be allowable considering the corresponding measurement repeatability. It was noted that optical transmission never failed throughout the tests, although the thermal expansion of the package material, stainless steel AISI 303, was considered to be less than the ideal and might cause fiber breaks. The slight bending of the fiber seemed to be effective in canceling the large thermal expansion mismatch. Further, the present new epoxy

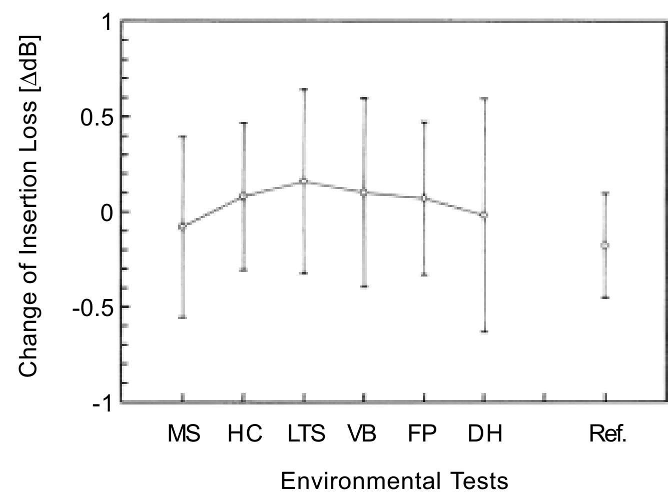

FIG. 4. Change of optical insertion losses (lightwave length = 1.55 µm) of the samples after the environmental tests. The initial insertion loss value was 3.6 dB on average (σ_{n-1} = 0.5 dB).

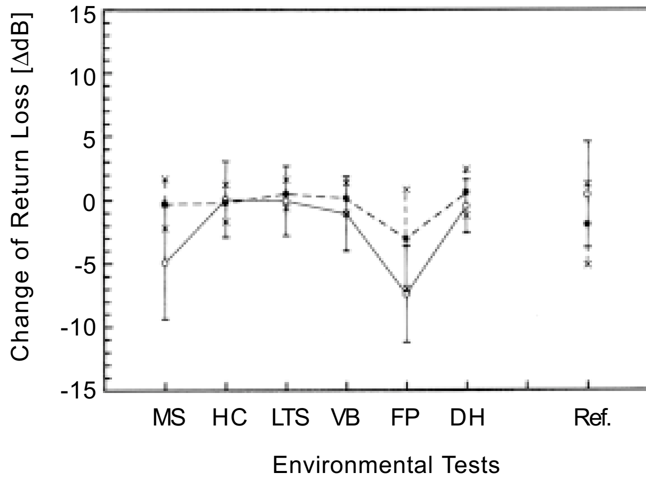

FIG. 5. Change of optical return losses of the samples after the environmental tests. Open and filled circled denote the results for input end and output end, respectively. The initial return loss value of the input side was 46 dB on average (σ_{n-1} = 3 dB). The initial return loss value of the output side was 48 dB on average (σ_{n-1} = 2 dB).

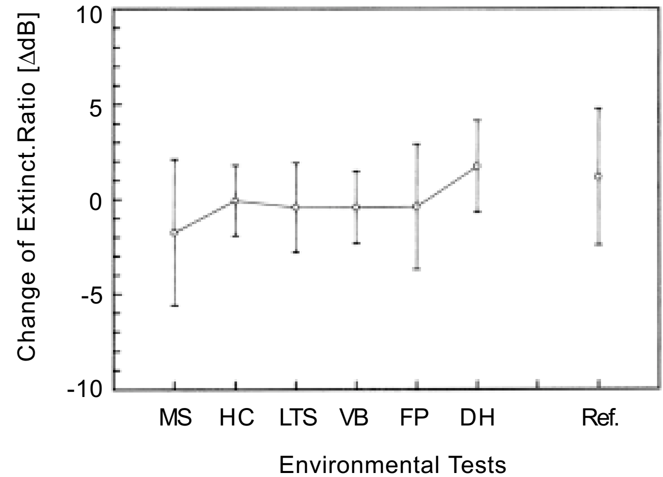

FIG. 7. Change of on/off extinction ratios of the samples after the environmental tests. The initial extinction ratio value was 25 dB on average (σ_{n-1} = 2 dB).

material "UV-1100" was found to resist thermal and mechanical shocks.

5. RESULTS OF THE DAMP HEAT TEST

The changes of optical insertion loss, return loss, V_π, extinction ratio, and interelectrode resistance during the damp heat test are revealed in Figs. 9 to 13. The measurements were done at 40°C and 95%RH and only the dc bias application was interrupted for the purpose of measurement. After the measurement, the dc bias was supplied again until the next measurement. During the damp heat storage for 56 days, no short circuit was observed for the modulator samples. When unsealed modulators were tested, an electrochemical reaction was generated between electrodes leading to a short circuits within a day. Concerning the parameters shown in Figs. 9-13, no significant deterioration was observed during storage. These unfailed samples were previously exposed under thermal and mechanical shocks, indicating that the ordinary magnitude of shocks did not cause significant moisture leaks at interfaces of the fiber, solder and stainless steel.

6. THERMAL AGING DURABILITY

To investigate the durability of the epoxy "UV-1100" fiber after coupling, four different modulators were aged at 85°C

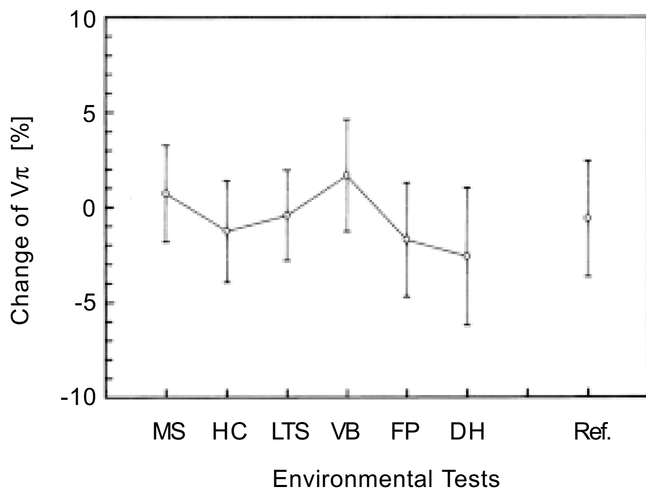

FIG. 6. Change of $V_\pi$ís of the samples after the environmental tests. The initial V_π value was 3.4 V on average (σ_{n-1} = 0.07 V).

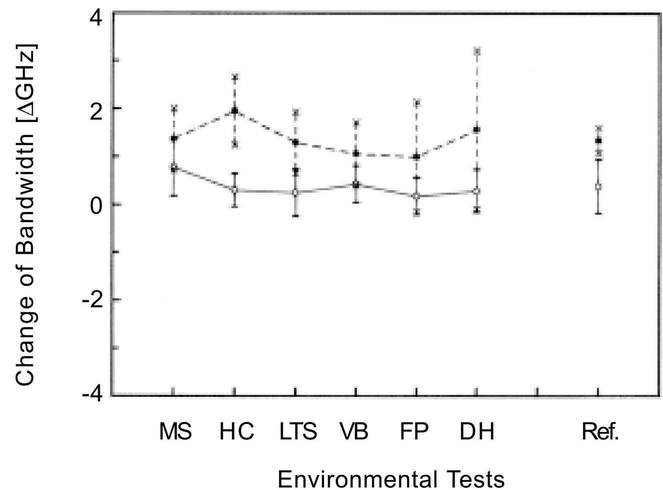

FIG. 8. Change of electrical (open circles) and optical (filled circles) bandwidths of the samples after the environmental tests. The initial electrical bandwidth value was 4.6 GHz on average (σ_{n-1} = 0.4 GHz). The initial optical bandwidth value was 8.6 GHz on average (σ_{n-1} = 1.5 GHz).

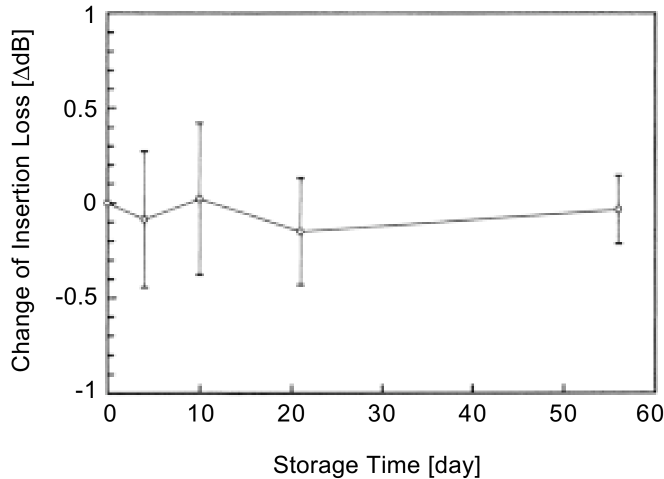

FIG. 9. Change of optical insertion losses of the samples during the damp heat test at 40°C and 95%RH. The initial insertion loss value was 3.6 dB on average (σ_{n-1} = 0.8 dB).

for 5000h. After this test, too, no modulator failed and the changes of the parameters were small: 0.46 ± 0.08 ΔdB for the optical insertion loss, 0.22 ± 5.36 ΔdB for optical return loss, 1.2 ± 2.9% for V_{π}, -1.2 ± 4.0 ΔdB for extinction ratio, -0.35 ± 0.44 ΔGHz for electrical, and 0.16 ± 0.62 ΔGHz for optical bandwidths. Further, the remaining 11 modulators were baked at 80°C for 15 h under 5 mTorr atmosphere before the sealing process to reduce the internal moisture of the packages. Even after such a vacuum baking process, the change of optical insertion loss was only 0.24 ± 0.39 ΔdB. These results suggests that the present epoxy adhesive was acceptable for practical usage with high a mechanical reliability.

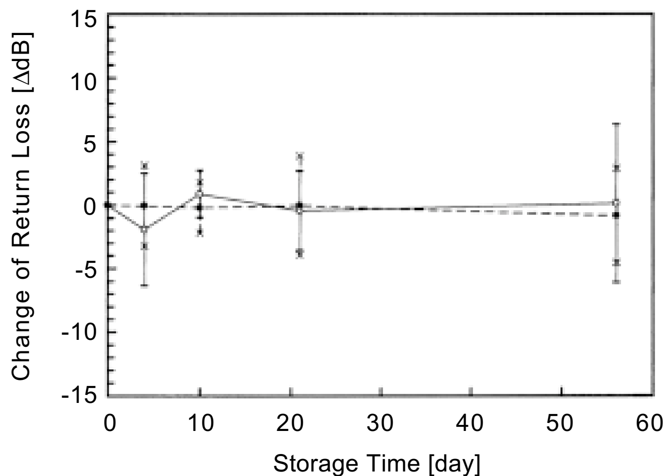

FIG. 10. Change of optical return losses of the samples during the damp heat test at 40°C and 95%RH. Open and filled circled denote the results for input end and output end, respectively. The initial return loss value of the input side was 47 dB on average (σ_{n-1} = 5 dB). The initial return loss value of the output end was 49 dB on average (σ_{n-1} = 4 dB).

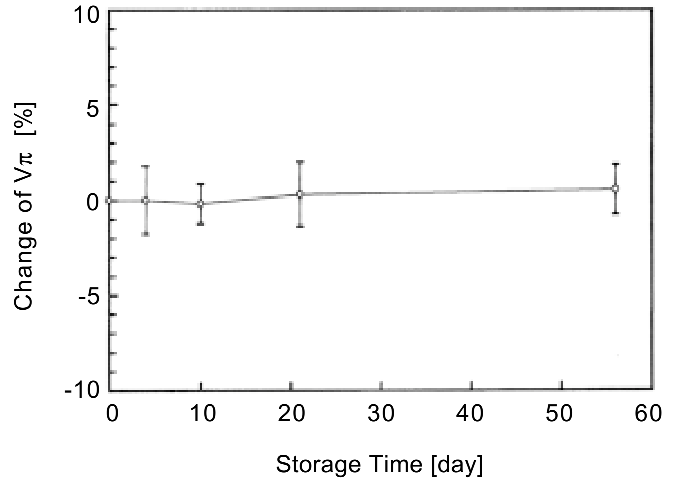

FIG. 11. Change of V_{π}ís of the samples during the damp heat test at 40°C and 95%RH. The initial V_{π} value was 3.3 V on average (σ_{n-1} = 0.07 V).

7. PACKAGE HERMETICITY

Figures 14 to 16 show He equivalent leak rates of the various packages measured before and after the temperature cycle and thermal shock tests. Concerning the hermeticity of the seam-welded stainless steel lids, no leak was detected, even after the environmental tests, as shown in Fig. 14, and kept less than 5 × 10^{-8}atm•cm^3/s of the leakage criterion mentioned in MIL-STD-883, 1014.9 for packages having large volume.

Figure 15 shows a leak from the rf-connector glass beads soldered to the package. Almost all samples could endure the environmental tests except for one sample (not shown in the figure). The leak rate of this failed sample increased from 8.4 × 10^{-8} to 1.4 × 10^{-6}atm•cm^3/s after the temperature shocks. By a scanning electron microscopic observation on the cross

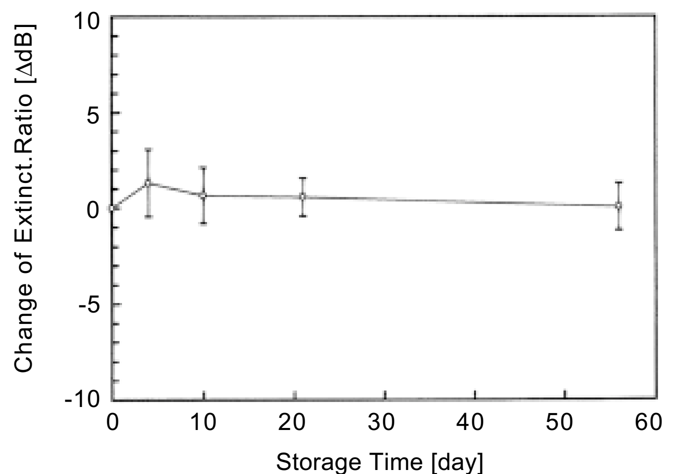

FIG. 12. Change of on/off extinction raios of the samples during the damp heat test at 40°C and 95%RH. The initial extinction raio value was 26 dB on average (σ_{n-1} = 2 dB).

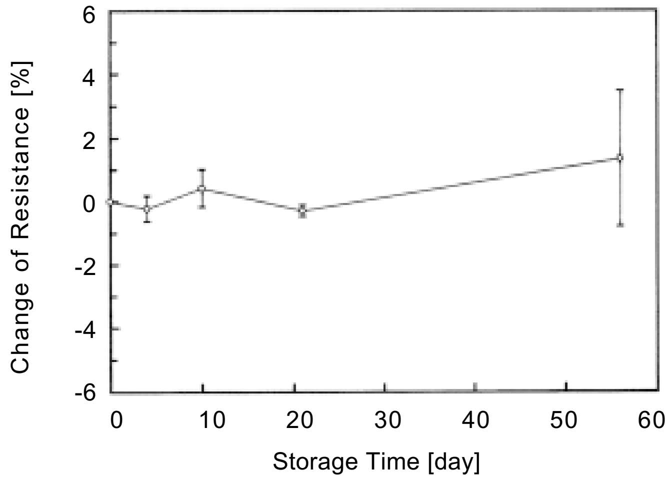

FIG. 13. Change of interelectrode resistances of the samples during the damp heat test at 40°C and 95%RH.

section of the failed portion, a separation at the interface between the electrode pin and the surrounding glass material was revealed as the probable path for the He leak. However, because the applied temperature shock, Δ180°C between -55 and 125°C, was considerably larger than the temperature range for device storage (-40-70°C), the present failure probability of 1/10 was considered to be very small for practical device operation. Similar tests for another 10 samples with improved electrode pins which were test-supplied from the manufacturer could not find any failures in the He leak. It was concluded that the use of a stainless-steel package was not disadvantageous for the installation of the commercial SMA connectors made from glass and Kovar.

The hermeticity of the fiber sealing portion also seemed to

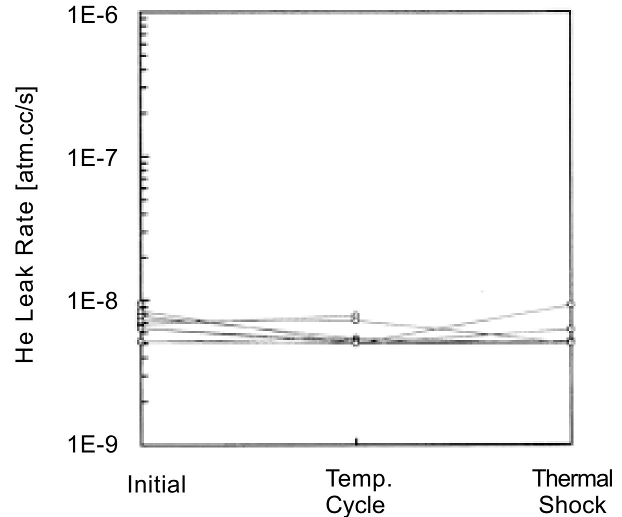

FIG. 15. He equivalent leak rates of the packages with seam-welded lids and soldered rf-connector glass beads, measured before and after the temperature cycle and thermal shock tests.

be allowable as shown in Fig. 16. Only 1 of the 9 samples failed due to such a severe test. Concerning the fiber sealing, however, a large leak over 1×10^{-6}atm•cm^3/s was sometimes detected in the as-prepared samples. Here, 3 samples, showing large leaks, had been rejected before the tests from the 12 prepared samples by the He leak screening.

In the present fiber-soldering procedure, the glass fiber surface was metallized with an inner Ni and outer Au layers by a conventional electroless plating method. The nominal layer thickness was ~ 0.3 µm for the Au layer and ~ 1 µm for the Ni. Figures 17a and 17b show a chemical depth profile of

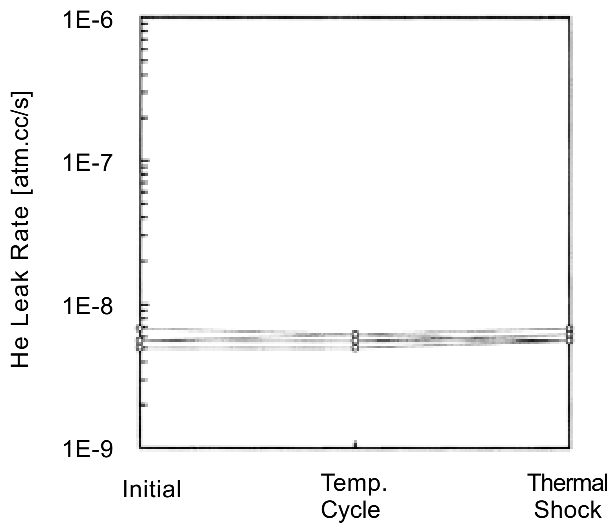

FIG. 14. He equivalent leak rates of the packages with seam-welded lids, measured before and after the temperature cycle and thermal shock tests.

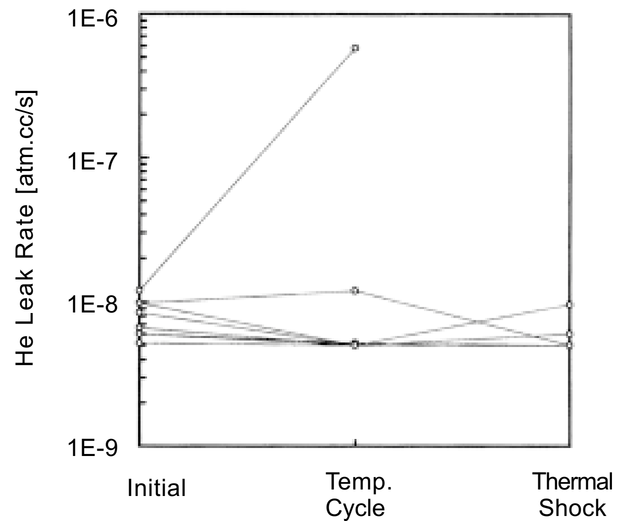

FIG. 16. He equivalent leak rates of the packages with seam-welded lids and soldered fibers, measured before and after the temperature cycle and thermal shock tests.

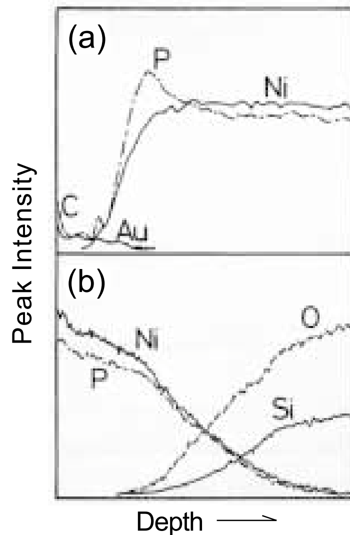

FIG. 17. AES depth profiles near (a) Au/Ni interface and (b) Ni/fiber interface of the electroless plated fiber. The left side of (a) denotes the metallized fiber surface.

the metallized layers measured by Auger electron spectroscopy(AES), where the regions near the Au surface and Au/Ni interface (Fig. 17a) and the Ni/SiO_2 interface (Fig. 17b) were revealed. The horizontal axis of the figure was not calibrated by the difference of Ar ion etching yields of the materials. The P in the Ni layer was supplied from a reducing agent for precipitating metallic Ni layer, *i.e.*, Ni-P alloy was formed [9]. Throughout the Ni-P layer, no oxygen was detected by AES measurement. A micro X-ray photoelectron spectrometry (XPS) also revealed the absence of an oxidized layer at the Au/Ni interface, judging from a Ni 2*p*3/2 peaks observed at 852.8 eV for metallic Ni. The results indicated that the thin Au layer could keep the metallic Ni surface and promised a good solderbility of the metallized fiber. On the other hand, the Ni 2*p*3/2 peak near the Ni/SiO_2 interface was measured at 853.5 eV, suggesting the presence of NiO (853.8 eV) and a formation of chemical bonding at the fiber interface.

Figure 18 is an AES depth profile of a Sn/Pb-solder-coated metallized fiber, in which the thick solder layer was ion etched previously. The Au of the metallized layer diffused into the solder and could not be detected by the AES. The growth of a Ni-Sn alloy layer was found between the Sn-Pb alloy and the Ni(-P) layers. The X-ray diffraction pattern of the soldered fiber revealed the existence of Ni_3Sn and Ni_3Sn_4 phases. A boundary between such Ni-Sn alloy layer and the Ni is known to be a possible origin for crack growth [10]. Concerning the present package samples showing a large He leak from the sealed fibers, a cross section of the fiber feed-through was investigated and two types of failure were found, crack growth at the solder/Ni interface and at the Ni/fiber interface, as expected. However, in the production process, such failed modulator products can be rejected via the He leak test be-

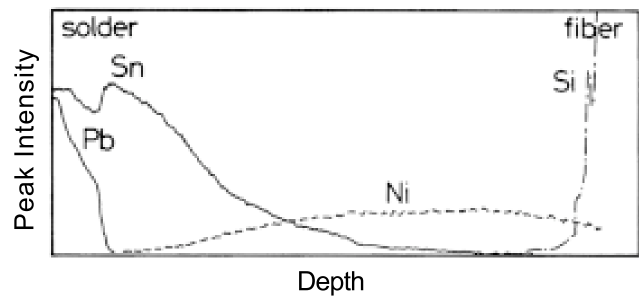

FIG. 18. AES depth profile of the electroless plated fiber after solder-dipping.

fore delivery, although further improvements in the fiber sealing are needed from the view point of achieving higher reliability and production yield.

8. CONCLUSION

Hermetically sealed 10 Gb/s LN optical modulators using new packaging materials were proposed for application in practical optical communication systems. The modulators were produced via volume-manufacturing processes and evaluated on their mechanical integrity. The results showed no deterioration in the optoelectrical characteristics and the package hermeticity, even after the environmental tests demanded in Bellcore's requirement TR-NWT-000468.

ACKNOWLEDGEMENTS

The authors thank the many staff members for the device fabrication, Dr.E.Min and Mr.M.Yaginuma of Sumitomo Osaka Cement Co., Ltd., for help in AES and XRD measurements of the metallized fibers, and also Dr.A.Kumar and the staff members of Seal Laboratory, CA, USA, for assistance in fine-leak tests and XPS measurements of the fiber.

REFERENCES

[1] A. O'Donnell, "Packaging and reliability of active integrated optical components," in *Proc. 7th Eur. Conf. on Int. Opt. (ECIO '95)*, p. 585, 1995.

[2] "Optical company focuses on AIM," *Electronics Times*, no. 794, 1996.

[3] P. G. Suchoski, Jr., and G. R. Boivin, "Reliability and accelerated aging of $LiNbO_3$ integrated optic fiber gyro circuits," in *Fiber Optic and Laser Sensors X, SPIE*, vol. 1795, p. 38, 1992.

[4] H. Nagata, M. Shiroishi, Y. Miyama, N. Mitsugi, and N. Miyamoto, "Evaluation of new uv-curable adhesive material for stable bonding between optical fibers and waveguide devices: problems in device packaging," *Opt. Fiber Technol.,* vol.1, 283 (1995).

[5] H. Nagata, H. Takahashi, H. Takai, and T. Kougo, "Impurity evaluations of SiO_2 films formed on $LiNbO_3$ substrate," *Jpn. J.Appl.Phys.*, vol. 34, 606 (1995).

[6] H. Nagata, and J. Ichikawa, "Progress and problems in reliability of Ti:$LiNbO_3$ optical intensity modulators," *Opt. Engineering*, vol. 34, 3284 (1995).

[7] N. Mitsugi, H. Nagata, M. Shiroishi, N. Miyamoto, and R. Kaizu,

"Otical fiber breaks due to buckling: Problems in device packaging," *Opt. Fiber Technol.*, vol. 1, 278 (1995).

[8] H. Nagata, N. Mitsugi, M. Shiroishi, T. Saito, T. Tateyama, and S. Murata, "Elimination of optical fiber breaks in stainless-steel packages for $LiNbO_3$ optical modulator devices," *Opt. Fiber Technol.*, vol. 2, 98 (1996).

[9] H. Tadao, M. Matsuoka, and H. Nawafune, Eds, *Mudenkai-Mekki (Electroless Plating)*, Chaps. 1-4, Nikkan Kogyo Shinbun-sha, Tokyo, 1994. [in Japanese].

[10] T. Takemoto and R. Satou, *Koushinraisei-Maikurosorudaringu-Gijyutsu (Highly Reliable Micro-soldering Technology)*, Kogyo Chousa-Kai, Tokyo, 1991. [in Japanese].